



## Drift-flux model in a sub-channel of rod bundle geometry

J. Enrique Julia<sup>a</sup>, Takashi Hibiki<sup>b,\*</sup>, Mamoru Ishii<sup>b</sup>, Byong-Jo Yun<sup>c</sup>, Goon-Cherl Park<sup>d</sup>

<sup>a</sup>Departamento de Ingeniería Mecánica y Construcción, Universitat Jaume I, Campus de Riu Sec, 12071 Castellon, Spain

<sup>b</sup>School of Nuclear Engineering, Purdue University, 400 Central Dr., West Lafayette, IN 47907-2017, USA

<sup>c</sup>Thermal-hydraulics Research Center, Korea Atomic Energy Research Institute, Taejeon 305-600, South Korea

<sup>d</sup>Department of Nuclear Engineering, Seoul National University, Seoul 151-742, South Korea

### ARTICLE INFO

#### Article history:

Received 12 November 2007

Accepted 20 February 2009

Available online 28 March 2009

#### Keywords:

Drift-flux model  
Rod bundle  
Sub-channel  
Subcooled boiling flow  
Void fraction  
Drift velocity

### ABSTRACT

In view of the practical interest of the drift-flux model for two-phase flow analysis, the distribution parameter and drift velocity constitutive equations have been obtained for subcooled boiling flow in a sub-channel of rod bundle geometry. The constitutive equation of the distribution parameter for subcooled boiling flow in a sub-channel is obtained from the bubble-layer thickness model. In this derivation an existing constitutive equation for subcooled boiling flow in a round pipe is modified by taking account of the difference in the flow channel geometry between the sub-channel and round pipe. The constitutive equation of the drift velocity is proposed based on an existing correlation and considering the rod wall and sub-channel geometry effects. The prediction accuracy of the newly developed correlations has been checked against experimental data in a  $3 \times 3$  rod bundle sub-channel, obtaining better predicting errors than the existing correlations most used in literature.

© 2009 Elsevier Ltd. All rights reserved.

### 1. Introduction

There is an increasing interest in both academia and industry in a variety of engineering systems concerning two-phase flows for their optimum design and safe operations. Among them, the modeling of the two-phase flow in a sub-channel is of great importance to the safety analysis of nuclear power plants and verification of thermal-hydraulic design codes. This fact is especially important in boiling water nuclear reactors (BWRs) since the two-phase flow is involved in its standard operational conditions [1].

Nowadays, drift-flux model [2–4] is widely used to predict the two-phase flow behavior in multiple scenarios. Its importance relies on its simplicity and applicability to a wide range of two-phase flow problems of practical interest. In the drift-flux model, two constitutive relations are needed to close the mathematical formulation and solve the problem. In this regard, distribution parameter and drift velocity need to be obtained by appropriate constitutive equations.

Recently, several works have been developed to obtain sound and accurate distribution parameter and drift velocity constitutive equations based on extensive dataset and mechanistic models in different flow conditions [4–7]. A complete review of the available constitutive equations can be found in [4]. However, most of the studies mentioned above were concentrated on flows in round tube geometry because, in spite of its simplicity, it is involved in many practical applications. Though, in many of the nuclear sys-

tems, more complex geometries like separators, fuel bundles and steam generators are present. Often, studies performed on simple geometries are not sufficient for the modeling needs in these complex geometries. This fact is especially important in the case of the drift-flux modeling in rod bundle sub-channel geometries, since many of the actual computational thermohydraulic code calculations are based on the drift-flux model.

Available distribution parameter and drift velocity constitutive equations developed for rod bundle geometries are empirical correlations that have been derived from rod bundle data (mainly differential pressure measurements) and have been tested against different rod bundle databases [8] in a wide range of void fraction conditions.

Bestion [9] developed a correlation to be used in the thermalhydraulic code CATHARE. The correlation is based on experimental data in rod bundles with hydraulic diameters of 12 mm and 24 mm and also the visual observations given by Venkateswararao et al. work [10]. The Bestion's work [9] only provides the drift velocity correlation, thus a constant distribution parameter of unity has been assumed since it provides the most accurate results compared to the experimental datasets available in literature [8].

Chexal et al. [11] developed a distribution parameter correlation based on the Zuber–Findlay's drift-flux model [2] and the main modifications are focused on the distribution parameter. In their work, Chexal et al. developed correlations for both upward and downward flows in vertical, inclined and horizontal pipes with different fluid types. In the case of upward water-steam flow in a vertical pipe, the distribution parameter and drift velocity

\* Corresponding author. Tel.: +1 765 496 9033; fax: +1 765 494 9570.  
E-mail address: [hibiki@purdue.edu](mailto:hibiki@purdue.edu) (T. Hibiki).

**Nomenclature**

*A* coefficient  
*A<sub>C</sub>* flow channel area  
*A<sub>wp</sub>* bubble layer area  
*B<sub>sf</sub>* bubble size factor  
*C<sub>0</sub>* distribution parameter  
*C<sub>0,Ishii</sub>* distribution parameter given by Ishii's equation for boiling flow in a round tube  
*C<sub>0,∞</sub>* asymptotic value of distribution parameter  
*D<sub>0</sub>* rod diameter  
*D<sub>b</sub>* bubble diameter  
*D<sub>H</sub>* hydraulic diameter  
*D<sub>Sm</sub>* Sauter mean diameter  
*G* mass flow rate  
*j* mixture superficial velocity  
*n* exponent  
*p* pressure  
*p<sub>crit</sub>* critical pressure  
*P<sub>0</sub>* pitch distance  
*Q* heat flux  
*Re<sub>b</sub>* bubble Reynolds number  
*Re<sub>∞</sub>* bubble Reynolds number in single-bubble system  
*R<sub>p</sub>* radius of round tube  
*R<sub>0</sub>* rod radius  
*r* radial coordinate measured from rod surface  
*T* temperature  
*v<sub>g</sub>* interfacial velocity  
*v<sub>f</sub>* liquid velocity  
*v<sub>gj</sub>* drift velocity

*v<sub>r</sub>* relative velocity  
*v<sub>r∞</sub>* bubble terminal velocity  
*x<sub>wp</sub>* bubble-layer thickness

*Greek symbols*

*α* void fraction  
*α<sub>wp</sub>* void fraction at assumed square void peak  
*ΔT<sub>sub</sub>* liquid subcooling  
*A* modification factor  
*ν* kinematic viscosity  
*ρ* density  
*σ* surface tension

*Subscripts*

*g* gas phase  
*f* liquid phase  
*in* inlet  
*sub* subcooled

*Mathematical symbols*

*⟨⟩* area averaged value  
*⟨⟨⟩* void-fraction-weighted mean value

*Acronyms*

BWR boiling water reactor  
 LSTF light water high conversion reactor  
 THTF thermal hydraulic test facility  
 TPTF two-phase flow test facility

correlations are those known as the EPRI correlation that were developed by the same authors in 1986 [12]. In addition, the critical pressure parameter is introduced in the distribution parameter equation.

Later, Inoue et al. [13] developed a distribution parameter correlation based on the Zuber–Findlay's drift-flux model that was derived from void fraction data in an 8 × 8 BWR facility [14]. Thus, the distribution parameter and drift velocity correlations were obtained by experimental data fitting and taking the inlet pressure and mass flux as working parameters.

Finally, Maier and Coddington [15] extended the correlation obtained by Inoue et al. to a wider range of experimental conditions

and flow configurations. The explicit correlations for all the constitutive equations used in these models are given in Table 1.

In the existing works, modeled distribution parameter and drift velocity were evaluated by one-dimensional data. There are very limited attempts to develop mechanistic drift-flux model considering phase distribution and channel geometry effect and to validate them with local flow parameters such as local void fraction and gas and liquid velocities. In this paper, new constitutive equations for the drift-flux model developed for subcooled boiling bubbly flow in a sub-channel of rod bundle geometry are presented. It will be shown that the constitutive equation of the distribution parameter

**Table 1**  
Existing drift-flux models applicable to bundle or sub-channel test sections.

Authors	<i>C<sub>0</sub></i> expression	<i>⟨⟨v<sub>gj</sub>⟩⟩</i> expression	Applicable range	Ref.
Bestion (1990)	<i>C<sub>0</sub></i> = 1	<i>⟨⟨v<sub>gj</sub>⟩⟩</i> = 0.188 √(g <i>D<sub>H</sub>ΔT<sub>sub</sub></i> /ρ <sub>g</sub> )	Whole range	[9]
Chexal–Lellouche (1992)	<i>C<sub>0</sub></i> = $\frac{L}{K_0 + (1 - K_0)2^x}$  $L = \frac{1 - e^{-C_1}}{1 - e^{-C_1} - C_1}$ , $C_1 = \frac{4p_{crit}^2}{p(p_{crit} - p)}$  $K_0 = B_1 + (1 - B_1)\left(\frac{\rho_g}{\rho_f}\right)^{1/4}$ , $r = \frac{1 + 1.57\left(\frac{\rho_g}{\rho_f}\right)}{1 - B_1}$  $B_1 = \min\left(0.8, \frac{1}{1 + e^{-Re_f/60000}}\right)$ , $Re = \max(Re_f, Re_g)$	<i>⟨⟨v<sub>gj</sub>⟩⟩</i> = 1.41 $\left(\frac{g\sigma\Delta\rho}{\rho_f^2}\right)^{1/4} C_2 C_3 C_4 C_9$  $C_2 = \begin{cases} 0.4757 \left(\ln\left(\frac{\rho_f}{\rho_g}\right)\right)^{0.7} & \text{if } \frac{v_{+f}}{\rho_g} \leq 18 \\ 1 & \text{if } C_5 \geq 1 \\ \left(1 - \exp\left(\frac{-C_5}{1 - C_5}\right)\right)^{-1} & \text{if } C_5 \leq 1 \text{ if } \frac{\rho_f}{\rho_g} > 18 \end{cases}$  $C_3 = \max\left(0.5, 2\exp\left(\frac{- Re_f }{60000}\right)\right)$  $C_4 = \begin{cases} 1 & \text{if } C_7 \geq 1 \\ \left(1 - \exp\left(\frac{-C_7}{1 - C_7}\right)\right)^{-1} & \text{if } C_7 < 1 \end{cases}$  $C_5 = \sqrt{150\frac{\rho_f}{\rho_g}}$ , $C_7 = \left(\frac{0.09144}{D_H}\right)^{0.6}$ , $C_9 = (1 - \alpha)^{B_1}$	Whole range	[11]
Inoue et al. (1993)	<i>C<sub>0</sub></i> = 6.76 × 10 <sup>-3</sup> <i>p</i> + 1.026	<i>⟨⟨v<sub>gj</sub>⟩⟩</i> = (5.1 × 10 <sup>-3</sup> <i>G</i> + 6.91 × 10 <sup>-2</sup> ) × (9.41 × 10 <sup>-2</sup> <i>p</i> <sup>2</sup> - 1.99 <i>p</i> + 12.6)	Whole range	[13]
Maier and Coddington (1997)	<i>C<sub>0</sub></i> = 2.57 × 10 <sup>-3</sup> <i>p</i> + 1.0062	<i>⟨⟨v<sub>gj</sub>⟩⟩</i> = (6.73 × 10 <sup>-7</sup> <i>p</i> <sup>2</sup> - 8.81 × 10 <sup>-5</sup> <i>p</i> + 1.05 × 10 <sup>-3</sup> ) <i>G</i> + (5.63 × 10 <sup>-3</sup> <i>p</i> <sup>2</sup> - 1.23 × 10 <sup>-1</sup> <i>p</i> + 0.8)	Whole range	[15]

for subcooled boiling flow in a sub-channel is obtained from the bubble-layer thickness model proposed by Hibiki et al. [16]. In this derivation an existing constitutive equation for subcooled boiling flow in a round pipe [3] is modified by taking account of the difference in the flow channel geometry between the sub-channel and round pipe. In the case of the drift velocity, the correlation proposed by Ishii [3] for round pipes will be modified to work in subcooled boiling bubbly flow in a rod bundle sub-channel. The accuracy of the newly developed correlations has been confirmed with the data provided by Yun et al. [17] in a  $3 \times 3$  rod bundle sub-channel as well as with other published correlations. Yun et al. [17] database is the only one which provides local measurements of gas and liquid phases in a rod bundle sub-channel and, thus, can be used to determine both, distribution parameter and drift velocity, directly.

## 2. Experimental databases

Most of the existing experimental datasets in rod bundle geometry only provide void fraction data. In most of the published works the void fraction measurements were performed using differential pressure transducers. In some cases, more sophisticated techniques such as X-ray tomography [14,18] and  $\gamma$  densitometry [19] were used. Very limited local data of gas and liquid flow parameters are available for boiling flow in rod bundle geometry [17]. A detailed list of the experimental datasets is given in Table 2.

In this regard, only the local data given by Yun et al. [17] is available in rod bundle sub-channels. The experiments were carried out in a  $3 \times 3$  rod bundle assembly (see Fig. 1(a) using a Pitot tube and a double-sensor conductivity probe to obtain the local flow parameters in liquid and gas phases, respectively. The hydraulic diameter of the rod bundle measured sub-channel,  $D_H$ , is 34.6 mm. The measured flow parameters include the void fraction, interfacial area concentration, bubble diameter, gas velocity and liquid velocity. The measurements were performed at 20 different locations (Fig. 1(b) in one of the sub-channels, i.e., center sub-channel with area-averaged void fraction  $\langle \alpha \rangle$  values up to 0.2 and a mass flow rate, heat flux, inlet temperature and subcooled temperature ranges of 250–522 kg/m<sup>2</sup>s, 25–185 kW/m<sup>2</sup>, 96.6–104.9 °C and 2–11 K, respectively. This dataset can provide useful information such as the phase distribution and mixture volumetric flux profiles inside the sub-channel. In the data base, the data at low void fraction ( $\langle \alpha \rangle < 0.01$ ), whereas it is known that the distribution parameter at the limiting condition ( $\langle \alpha \rangle = 0$ ) to be zero [3,4]. Thus it is possible to obtain the distribution parameter between the limiting condition ( $\langle \alpha \rangle = 0$ ) and high void fraction ( $\langle \alpha \rangle = 0.2$ ).

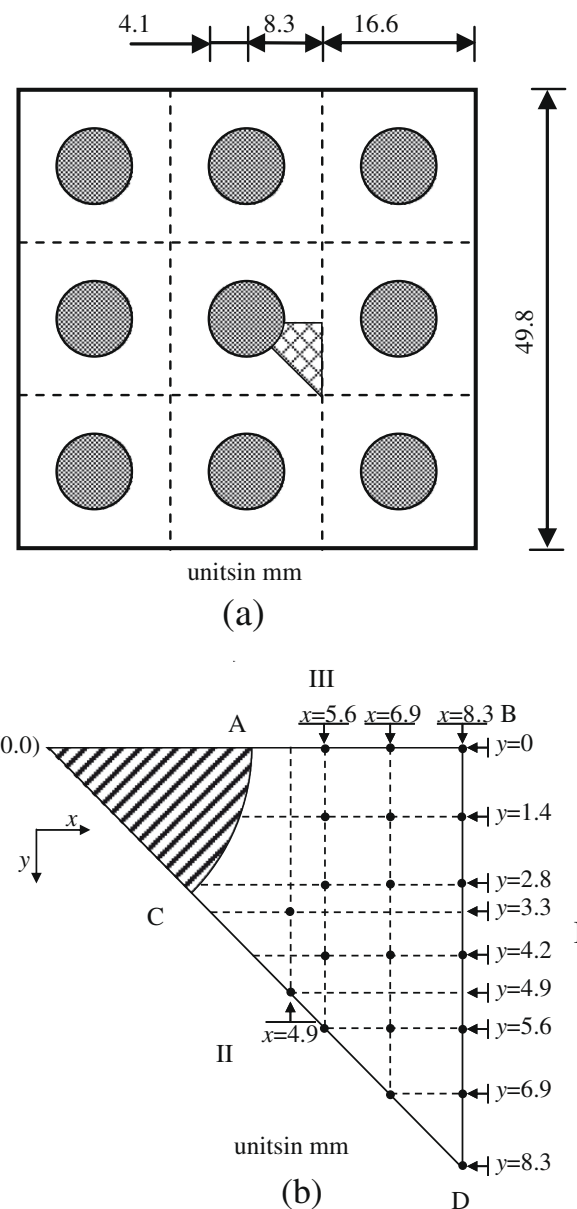


Fig. 1. (a) Schematic diagram of the  $3 \times 3$  rod bundle assembly used in the Yun et al. experiments [17]. (b) Detail of the considered sub-channel with the measured point locations.

Table 2  
Existing databases obtained in bundle or sub-channel test section.

Experimental facility	Type	Length (m)	Rods (heated)	$D_H$ (mm)	$D_0$ (mm)	Axial power distribution	$\Delta T_{sub}$ (K)	$p$ (Mpa)	$G$ (Kg/m <sup>2</sup> s)	$q$ (kW m <sup>-2</sup> )	No. flow cond.	Measured parameters	Measurement technique	Ref.
PERICLES (1985)	PWR	3.7	357 (357)	9.5	11	Chopped cosine	20/60	0.3–0.6	21–48	11–40	21	$\langle \alpha \rangle$	DP transducers	[20]
NEPTUN (1988)	LWHCR	1.7	37 (37)	10.7	4	Chopped cosine	0.5/3	0.4	42/91	5/10	48	$\langle \alpha \rangle$	DP transducers	[21]
BWR 4 × 4 (1990)	BWR	3.7	16 (16)	12.3	12	Uniform	0	0.5/1	833/1390	350–743	20	$\langle \alpha \rangle$	X-ray tomography	[18]
BWR 8 × 8 (1991)	BWR	3.7	64 (62)	12.3	13	Uniform/chopped cosine	9–12	1–8.6	284–1988	225–3377	20	$\langle \alpha \rangle$	DP transducers and X-ray tomography	[14]
LSTF (1990)	PWR	3.7	1104 (1008)	9.5	13	Chopped cosine	0	1/7.3/15	2.2–84	5–45	14	$\langle \alpha \rangle$	DP transducers	[22]
TPTF (1994)	PWR	3.7	32 (24)	9.5	10	Uniform	5–35	3/6.9/11.8	11–189	9–170	18	$\langle \alpha \rangle$	$\gamma$ radiation and DP transducer	[19]
THTF (1982)	PWR	3.7	64 (60)	9.5	11	Uniform	46–118	3.9–8.1	3.1–29	11–74	11	$\langle \alpha \rangle$	DP transducers	[23]
Yun (1996)	BWR	1.7	9 (9)	18.4	8.2	Uniform	3.5–11	0.12	250–522	25–185	53	$\alpha$ , $a_i$ , $v_g$ , $D_{Sm}$ , $v_f$	Conductivity probe, Pitot tube	[17]

### 3. Modeling

#### 3.1. Drift-flux model

The drift velocity of a gas phase,  $v_{gj}$ , is defined as the velocity of the gas phase,  $v_g$ , with respect to the volume center to the mixture flux,  $j$

$$v_{gj} = v_g - j = (1 - \alpha)(v_g - v_f) = (1 - \alpha)v_r, \quad (1)$$

where  $v_f$ ,  $\alpha$  and  $v_r$  are the liquid velocity, void fraction and relative velocity between phases, respectively. The void-fraction-weighted mean drift velocity,  $\langle\langle v_{gj} \rangle\rangle$ , is given by

$$\langle\langle v_{gj} \rangle\rangle \equiv \frac{\langle\alpha v_{gj}\rangle}{\langle\alpha\rangle} = \frac{\langle\alpha v_g\rangle}{\langle\alpha\rangle} - \frac{\langle\alpha j\rangle}{\langle\alpha\rangle} = \frac{\langle j_g \rangle}{\langle\alpha\rangle} - \frac{\langle\alpha j\rangle}{\langle\alpha\rangle}, \quad (2)$$

where  $\langle \rangle$  means a simple area average and  $j_g$  is the gas superficial velocity. The one-dimensional drift-flux model can be derived by recasting Eq. (2) in terms of the distribution parameter,  $C_0$ , and the void-fraction-weighted mean drift velocity as

$$\langle\langle v_g \rangle\rangle \equiv \frac{\langle j_g \rangle}{\langle\alpha\rangle} = C_0 \langle j \rangle + \langle\langle v_{gj} \rangle\rangle, \quad (3)$$

where

$$C_0 \equiv \frac{\langle\alpha j\rangle}{\langle\alpha\rangle \langle j \rangle}. \quad (4)$$

#### 3.2. Distribution parameter

In 1977, Ishii [3] proposed a simple model for the distribution parameter for bubbly, slug and churn-turbulent flow in adiabatic flow given by

$$C_0 = C_{0,\infty} - (C_{0,\infty} - 1)\sqrt{\rho_g/\rho_f}, \quad (5)$$

in this equation  $\rho_g$  and  $\rho_f$  represent the gas and liquid phase densities, respectively, and  $C_{0,\infty}$  the asymptotic distribution parameter value for high void fraction.

Ishii extended the use of Eq. (5) to boiling flow by the addition of a weighting factor that takes into account the wall bubble nucleation and makes  $C_0 \rightarrow 0$  when  $\langle\alpha\rangle \rightarrow 0$ . In this case the distribution parameter is given by

$$C_0 = \left\{ C_{0,\infty} - (C_{0,\infty} - 1)\sqrt{\rho_g/\rho_f} \right\} (1 - e^{A\langle\alpha\rangle}), \quad (6)$$

where the coefficient  $A$  and  $C_{0,\infty}$  are recommended to be  $-18$  and  $1.2$  for round pipes, respectively.

It has been shown that the use of Eqs. (5) and (6) can be extended to other flow channel geometries if the parameters  $C_{0,\infty}$  and  $A$  are properly modified. Ishii [3] showed that the distribution parameter for adiabatic flow in a rectangular duct can be given by

$$C_0 = 1.35 - 0.35\sqrt{\rho_g/\rho_f}. \quad (7)$$

In addition, the distribution parameter for subcooled boiling flow in an internally heated annulus was obtained by Hibiki et al. [16]. In that work, the dependence of the distribution parameter with the area-averaged void fraction was obtained by a power fitting of the explicit form of the coefficient  $A$  given in Eq. (8) with the area-averaged void fraction.

$$A = \frac{1}{\langle\alpha\rangle} \ln \left( 1 - \frac{C_0}{C_{0,\infty} - (C_{0,\infty} - 1)\sqrt{\rho_g/\rho_f}} \right) \quad (8)$$

Thus, the constitutive equation for the distribution parameter in subcooled boiling in an internally heated annulus is given by

$$C_0 = \left( 1.2 - 0.2\sqrt{\frac{\rho_g}{\rho_f}} \right) \left( 1 - e^{-3.12\langle\alpha\rangle^{0.212}} \right) \quad (9)$$

Recently, Ozar et al. [24] work has shown analytically that  $C_{0,\infty}$  should be  $1.1$  in adiabatic flow in an annular channel instead of  $1.2$ . This result has been validated experimentally by detailed measurement of the liquid and gas phase velocity profiles. If these last findings are taken into account, Eq. (9) can be modified obtaining a new correlation for subcooled boiling in an internally heated annulus as

$$C_0 = \left( 1.1 - 0.1\sqrt{\frac{\rho_g}{\rho_f}} \right) \left( 1 - e^{-6.85\langle\alpha\rangle^{0.359}} \right). \quad (10)$$

In the present work, the distribution parameter for a sub-channel of rod bundle geometry has been derived. First the  $C_{0,\infty}$  value in a sub-channel can be obtained analytically by the use of Eq. (4) and the appropriate  $j$ - and  $\alpha$ -distributions at high void fraction condition. In order to obtain the complete  $C_0$  distribution, the Ishii's equation for boiling flow in a round pipe, Eq. (6), has been modified in order to take into account the flow channel geometry difference. The modification factor has been analytically obtained by the use of the bubble-layer thickness model [16].

As mentioned above, the asymptotic value of the distribution parameter can be approximated by Eq. (4), using mixture volumetric flux and void fraction profiles at high void fraction condition. For this purpose the analytical forms of the  $j$ - and  $\alpha$ -distributions are needed. The modeled sub-channel, including the coordinate system, is given in Fig. 2(a).

The mixture volumetric flux,  $j$ , is assumed by

$$j(r, \theta) = j_c(\theta) \left\{ 1 - \left( 1 - \frac{2r_0}{R - R_0} \right)^n \right\} \quad (0 \leq r_0 \leq R_c - R_0; 0 \leq \theta \leq \pi/4), \quad (11)$$

where  $r_0$  is the radial distance measured from the rod surface and  $j_c(\theta)$  is the mixture volumetric flux at a point on the line B.  $R_c$  is defined as the distance between the origin and the point of the intersection of the line A with line B,  $P_0$  is the distance between two rods (pitch) and  $R$  is defined as

$$R = 2R_c - R_0. \quad (12)$$

The cosine of the angle between  $x$ -axis and line A is given by

$$\cos \theta = \frac{P_0}{2R_c}. \quad (13)$$

Thus we have

$$R = \frac{P_0}{\cos \theta} - R_0. \quad (14)$$

It should be noted here that  $R$  ranges from  $P_0 - R_0$  to  $\sqrt{2}P_0 - R_0$ .

Eq. (11) indicates that the mixture volumetric flux along the line A is assumed to be a power law profile with its maximum value at  $(r, \theta) = (R_c, \theta)$ , namely at a point of the intersection of the line A with the line B and zero at  $(r, \theta) = (R_0, \theta)$ , namely at a point on the rod surface.

Substituting  $R$  in Eq. (11) with Eq. (14) yields

$$j(r, \theta) = j_c(\theta) \left\{ 1 - \left( 1 - \frac{2r_0 \cos \theta}{P_0 - 2R_0 \cos \theta} \right)^n \right\}. \quad (15)$$

Here,  $j_c$  is assumed by

$$j_c(\theta) = j_{c0} \left[ 1 - \left\{ 1 - \frac{P_0 - 2R_0 \cos \theta}{(\sqrt{2}P_0 - 2R_0) \cos \theta} \right\}^n \right], \quad (16)$$

where  $j_{c0}$  is the mixture volumetric flux at the center of the sub-channel as indicated by open square in Fig. 2(b), namely the

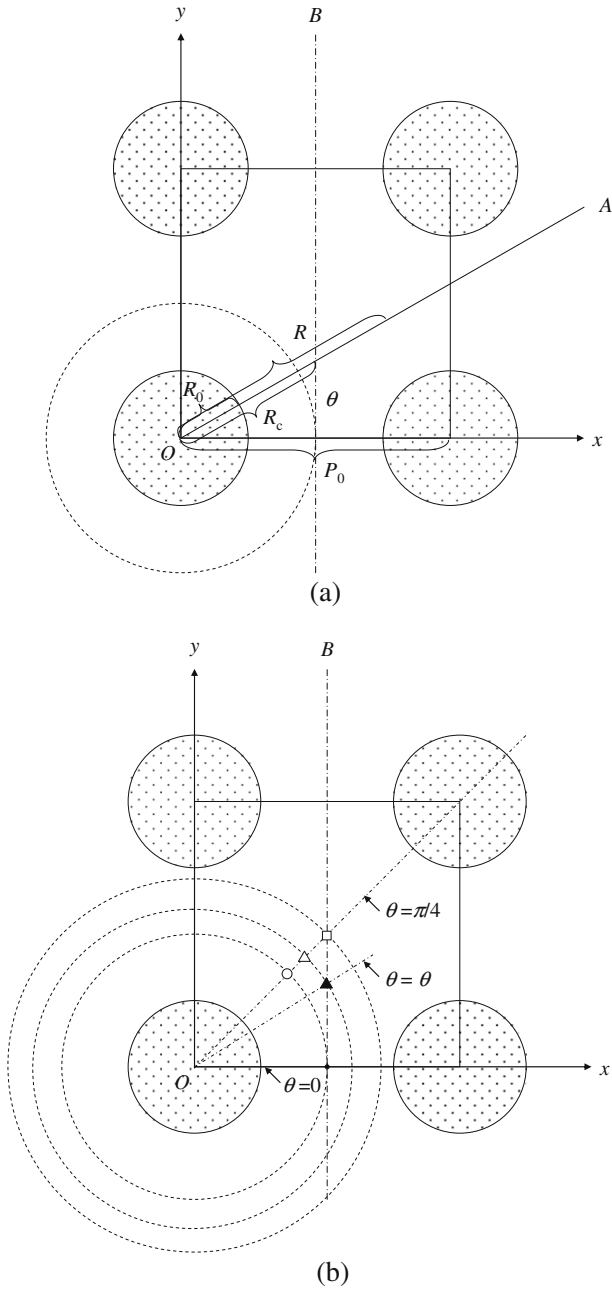


Fig. 2. (a) Modeled sub-channel including coordinate. (b) Physical meaning of assumed  $j_{c0}$ .

mixture volumetric flux at  $(r, \theta) = (P_0/\sqrt{2}, \pi/4)$ . Eq. (16) indicates that the maximum mixture volumetric flux on the line A, namely the mixture volumetric flux at a point of the intersection of the line A with the line B is assumed to be the same as the mixture volumetric flux at  $(r, \theta) = (R_c, \pi/4)$ . In other words, the mixture volumetric flux at a point indicated by solid triangle (or open triangle) in Fig. 2(b) is assumed to be the same as that at a point indicated by open triangle (or open triangle).

Finally, substituting  $j_{c0}$  in Eq. (16) with Eq. (14) yields

$$j(r, \theta) = j_{c0} \left[ 1 - \left\{ 1 - \frac{P_0 - 2R_0 \cos \theta}{(\sqrt{2}P_0 - 2R_0) \cos \theta} \right\}^n \right] \times \left\{ 1 - \left( 1 - \frac{2r_0 \cos \theta}{P_0 - 2R_0 \cos \theta} \right)^n \right\}, \quad (17)$$

where

$$0 \leq r_0 \leq \frac{P_0}{2 \cos \theta} - R_0 \quad (18)$$

and  $j_{c0}$  can be obtained by integrating  $j(r, \theta)$  over the flow channel.

In a similar way, the void fraction distribution for the adiabatic flow in the sub-channel can be defined as

$$\alpha(r, \theta) = \alpha_{c0} \left[ 1 - \left\{ 1 - \frac{P_0 - 2R_0 \cos \theta}{(\sqrt{2}P_0 - 2R_0) \cos \theta} \right\}^m \right] \times \left\{ 1 - \left( 1 - \frac{2r_0 \cos \theta}{P_0 - 2R_0 \cos \theta} \right)^m \right\}. \quad (19)$$

Thus, the asymptotic value of the distribution parameter can be calculated by using the Eq. (4) and Eqs. 17 and 19.

The modeled mixture volumetric flux is evaluated by existing data. Fig. 3(a and b) indicate the comparisons of modeled  $j/j_{c0}$  pro-

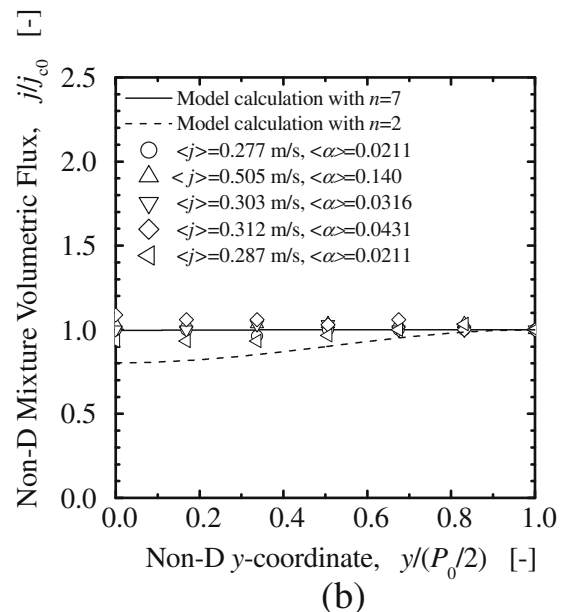
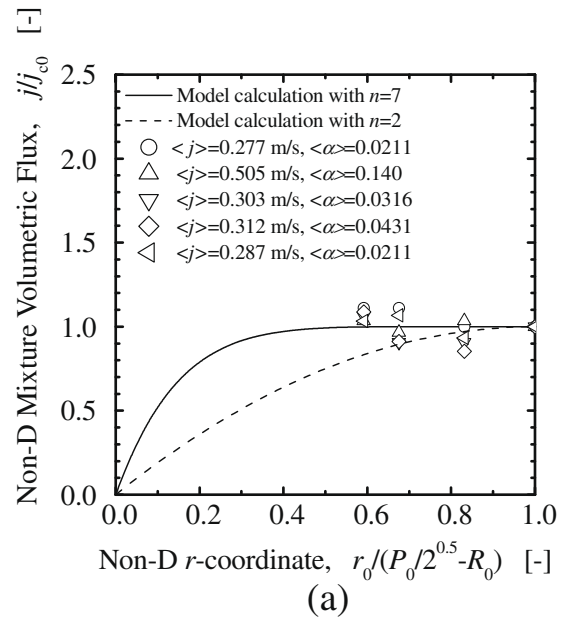


Fig. 3. Comparison of modeled  $j/j_{c0}$  profile with Yun et al. data [17] at (a)  $\theta = \pi/4$  and (b)  $r_0 = P_0/(2 \cos \theta) - R_0$ .

file at  $\theta = \pi/4$  and modeled  $j/j_{co}$  profile at  $r_0 = P_0/(2\cos\theta) - R_0$  with Yun et al. dataset [17], respectively. Since  $j$  profiles are normalized by a single measured data, namely  $j_{co}$ , the value of  $j/j_{co}$  is affected by the measured accuracy of  $j_{co}$ . In Fig. 3(a and b), the solid and broken lines indicate non-dimensional mixture volumetric flux calculated with  $n = 7$  and 2. These results support the validity of the assumed  $j$  profile for  $n = 7$ .

The calculated asymptotic values of distribution parameter in sub-channel as parameter of exponent,  $n$ , is shown in Fig. 4(a). In the calculation, the exponent for void fraction profile is assumed to be the same as that for mixture volumetric flux for simplicity and the non-dimensional rod diameter, defined as  $D_0/P_0$  (where  $D_0$  is the rod diameter), is 0.5. As shown in Fig. 4(a), as the exponent increases, or the mixture volumetric flux and void fraction profiles become flatter, the distribution parameter approaches 1.0. For  $n = 2$ , the distribution parameter reaches almost to 1.2, which is a typical value of the distribution parameter in a round pipe. However, in real two-phase flow in a sub-channel, the exponent may be around 7 as it was shown in Fig. 3. Unlike the case for a round pipe, the distribution parameter in sub-channel may be around 1.04, as pointed out by the experimental data [17]. Since  $\pm 30\%$  change of  $n$  only causes a  $\pm 1.5\%$  deviation from the value of

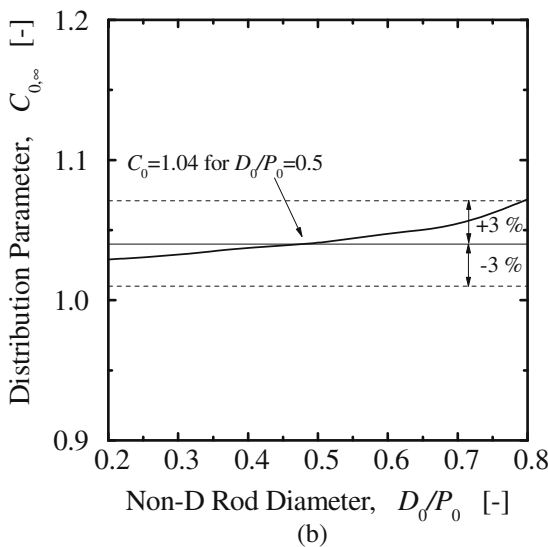
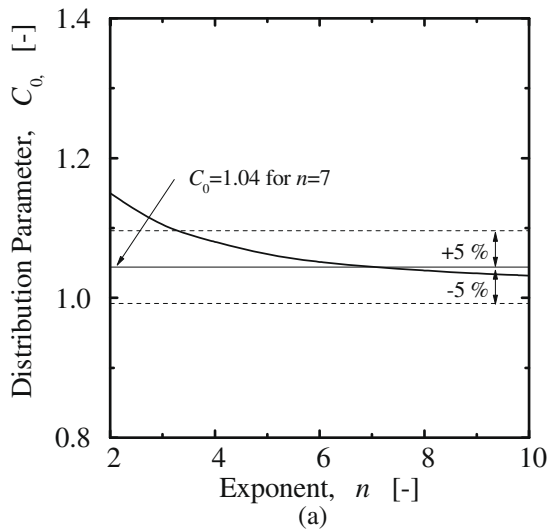


Fig. 4. Dependence of distribution parameter on (a) exponent  $n$  in  $j$ -distribution and (b) non-dimensional rod diameter  $D_0/P_0$ .

$C_{0,\infty}$  calculated by using  $n = 7$ , a slight change of  $n$  may not affect  $C_{0,\infty}$  significantly.

Fig. 4(b) shows the dependence of the asymptotic value of the distribution parameter with the non-dimensional rod diameter, using  $n = 7$  for the calculations. It is possible to observe that  $C_{0,\infty}$  increases with  $D_0/P_0$ . The dependence is weak for all the  $D_0/P_0$  range, but specially for  $D_0/P_0$  values below 0.7. If a value of 0.5 for  $D_0/P_0$  is chosen, that corresponds to  $C_{0,\infty}$  of 1.04, a maximum error of  $\pm 3\%$  is obtained for a rod bundle sub-channels with  $D_0/P_0$  values between 0.2 and 0.8 calculated by using a  $D_0/P_0$  value of 0.5. If more accuracy is needed, the following correlation obtained by a polynomial fitting of the data obtained in Fig. 4(b) can be used,

$$C_{0,\infty} = 1.002 + 0.206(D_0/P_0) - 0.438(D_0/P_0)^2 + 0.361(D_0/P_0)^3. \quad (20)$$

It should be noted here that the  $C_{0,\infty}$  values obtained by Eq. (20) may be also valid in slug and churn-turbulent flow regimes.

In order to obtain the complete distribution parameter correlation in the rod bundle sub-channel, the bubble-layer thickness model can be introduced to obtain the modified  $C_{0,\infty}$  and  $A$  parameters. The bubble-layer thickness model was successfully introduced by Hibiki et al. [16] in order to obtain the distribution parameter in an internally heated annulus. In this model, see Fig. 5, the subcooled flow path near a heated rod is divided into two regions, namely (i) boiling two-phase (bubble layer) region where the void fraction is assumed to be uniform and (ii) liquid single-phase region where the void fraction is assumed to be zero. In Fig. 5,  $\alpha$ ,  $x$ ,  $R_0$ ,  $\alpha_{wp}$ ,  $x_{wp}$  and  $R$  are the local void fraction, the radial coordinate measured from the center of the heater rod surface, the radius of the heater rod, the void fraction at the assumed void peak, the bubble-layer thickness, and the coordinate of the outer part of the considered sub-channel, respectively. Consequently, the void fraction distribution can be assumed as

$$\begin{aligned} \alpha &= \alpha_{wp} \quad \text{for } 0 \leq r \leq x_{wp}, \\ \alpha &= 0 \quad \text{for } x_{wp} \leq r \leq R - R_0 \end{aligned} \quad (21)$$

where the  $r$  coordinate is considered from the rod surface.

The distribution parameter for subcooled boiling flow in the sub-channel can be calculated using Eq. (4) and numerical integration of Eqs. 17 and 21. Unfortunately, no analytical solution can be obtained for the distribution parameter, so only numerical solutions will be provided in this work. Hibiki et al. [16] showed that the difference in the dependence of  $C_0$  on  $\langle \alpha \rangle$  between the round tube and other sub-channel geometries may mainly be attributed to the difference in the channel geometry. This assumption is valid for  $A_{wp}/A_C$  values lower than 0.3, where  $A_{wp}$  and  $A_C$  are the bubble and channel areas, respectively. Since the product of  $A_{wp}/A_C$  and  $\alpha_{wp}$  is equal to  $\langle \alpha \rangle$ ,  $A_{wp}/A_C$  may correlate closely with  $\langle \alpha \rangle$ . As a result, the distribution parameter for subcooled boiling flow in the rod bundle sub-channel can be obtained from Ishii's equation, Eq. (6), taking into account of the channel geometry effect on the distribution parameter as

$$C_0 = \Lambda \left( 1.2 - 0.2 \sqrt{\rho_g/\rho_f} \right) \left( 1 - e^{-18\langle \alpha \rangle} \right), \quad (22)$$

where  $\Lambda$  is the modification factor defined by the ratio of the distribution parameter for the sub-channel to that for the round tube for the same  $A_{wp}/A_C$  value given by

$$\frac{A_{wp}}{A_C} = \frac{\pi(x_{wp}^2 + D_0x_{wp})}{P^2 - \pi(D_0/2)^2} \quad \text{for rod bundle sub-channel} \quad (23)$$

$$\frac{A_{wp}}{A_C} = 1 - \left( 1 - \frac{x_{wp}}{R_p} \right)^2 \quad \text{for round tube} \quad (24)$$

where  $R_p$  is the radius of the round tube.

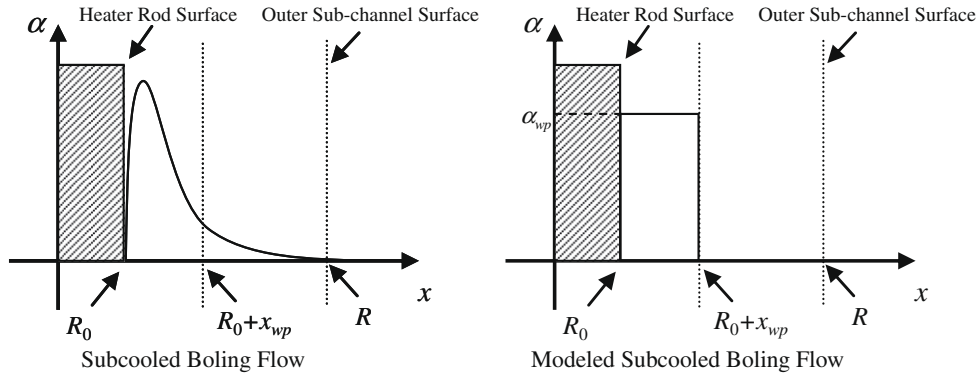


Fig. 5. Basic concept of bubble-layer thickness model.

In order to calculate the modification factor, the distribution parameter of boiling flow for a round tube is needed. Therefore, the void fraction and  $j$ -distributions are defined as [16]

$$\alpha = \alpha_{wp} \text{ for } R_p - x_{wp} \leq r \leq R_p, \quad (25)$$

$$\alpha = 0 \text{ for } 0 \leq r \leq R_p - x_{wp}$$

and

$$j = \frac{n+2}{n} \langle j \rangle \left\{ 1 - \left( \frac{r}{R_p} \right)^n \right\}. \quad (26)$$

From Eqs. (4), (25), and (26), we can obtain the distribution parameter for boiling flow in a round tube analytically as

$$C_0 = \frac{n - \left( 1 - \frac{x_{wp}}{R_p} \right)^2 \left\{ (n+2) - 2 \left( 1 - \frac{x_{wp}}{R_p} \right)^n \right\}}{n \left\{ 1 - \left( 1 - \frac{x_{wp}}{R_p} \right)^2 \right\}}. \quad (27)$$

Fig. 6 shows the modification factor obtained from Eq. (27) and the numerical integration of Eqs. (4), (17), and (21) as a function of the distribution parameter for the round tube and  $D_0/P_0$  values of 0.3, 0.5 and 0.7. In order to facilitate its use, the modification factor has been approximated to a polynomial function given by

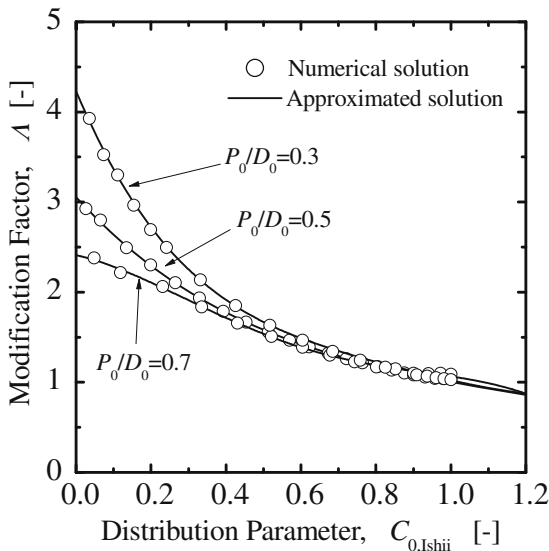


Fig. 6. Modification factor  $A$ .

$$A = \begin{cases} 4.229 - 10.043C_{0,Ishii}^2 + 14.282C_{0,Ishii} - 10.335C_{0,Ishii}^3 \\ \quad + 2.889C_{0,Ishii}^4 \text{ for } D_0/P_0 = 0.3 \\ 3.055 - 4.537C_{0,Ishii} + 4.033C_{0,Ishii}^2 - 1.882C_{0,Ishii}^3 \\ \quad + 0.335C_{0,Ishii}^4 \text{ for } D_0/P_0 = 0.5 \\ 2.412 - 0.896C_{0,Ishii} - 4.316C_{0,Ishii}^2 + 6.548C_{0,Ishii}^3 \\ \quad - 2.682C_{0,Ishii}^4 \text{ for } D_0/P_0 = 0.7 \end{cases} \quad (28)$$

It is possible to observe that the influence of the non-dimensional rod diameter value on the modification factor is more important for  $C_{0,Ishii}$  values lower than 0.5. The effect of the channel geometry in the distribution parameter has a larger impact for low void fraction conditions as reported by Hibiki et al. [16]. If higher  $C_{0,Ishii}$  values are considered the differences are insignificant. This fact can be easily explained by the small dependency of the  $C_{0,\infty}$  parameter with  $D_0/P_0$  (see Fig. 4(b)). If all the  $C_0$  range is considered, the modification factor equation for  $D_0/P_0 = 0.5$  can be used for a non-dimensional rod diameter range from 0.3 to 0.7 assuming a  $\pm 9\%$  error (calculated with respect to a  $D_0/P_0$  value of 0.5).

The results obtained by the use of the Eqs. (22) and (28) have been fitted to a equation with a similar functional form to those employed in previous works, see Eqs. (6), (9), and (10), and using a  $C_{0,\infty}$  values of 1.03, 1.04, and 1.05 corresponding to a  $D_0/P_0$  parameters of 0.3, 0.5 and 0.7, respectively (see Fig. 4(b)). Consequently, the newly developed distribution parameter correlation can be expressed, in a more condensed way, as,

$$C_0 = \begin{cases} \left( 1.03 - 0.03 \sqrt{\frac{\rho_g}{\rho_f}} \right) \left( 1 - e^{-26.3(\alpha)^{0.780}} \right) \text{ for } D_0/P_0 = 0.3 \\ \left( 1.04 - 0.04 \sqrt{\frac{\rho_g}{\rho_f}} \right) \left( 1 - e^{-21.2(\alpha)^{0.762}} \right) \text{ for } D_0/P_0 = 0.5 \\ \left( 1.05 - 0.05 \sqrt{\frac{\rho_g}{\rho_f}} \right) \left( 1 - e^{-34.1(\alpha)^{0.925}} \right) \text{ for } D_0/P_0 = 0.7 \end{cases} \quad (29)$$

### 3.3. Drift velocity

In order to obtain the drift velocity in the sub-channel, the constitutive equation developed by Ishii [3] for distorted-particle regime will be considered. This correlation has been chosen since it is a simple expression in which all the parameters needed are usually known and that has been successfully tested against different databases [3]. More sophisticated expressions can be found in literature, even developed for rod bundle sub-channels [25]. Though, these expressions need some input parameters such as some experimental data usually unavailable in rod bundle experiments like bubble diameter and aspect ratio. In this work, the expression

developed by Ishii [3] has been modified by considering the bubble size factor, and the final expression is given as

$$\langle\langle v_{gi} \rangle\rangle = B_{sf} \sqrt{2} \left( \frac{\sigma \Delta \rho g}{\rho_f^2} \right)^{1/4} (1 - \langle \alpha \rangle)^{1.75}, \quad (30)$$

where  $\sigma$ ,  $\Delta \rho$ ,  $g$  and  $B_{sf}$  are the surface tension, density difference between the phases, gravitational acceleration and the bubble size factor, respectively. The bubble size factor,  $B_{sf}$ , should be included in order to consider the rod wall effect in the bubble rising velocity. In this work, the reduction factor proposed by Wallis [26] will be used since it has been successfully used in rod bundle geometries [27].

$$B_{sf} = \begin{cases} 1 - \frac{D_b}{0.9L_{max}} & \text{for } \frac{D_b}{L_{max}} < 0.6 \\ 0.12 \left( \frac{D_b}{L_{max}} \right)^{-2} & \text{for } \frac{D_b}{L_{max}} \geq 0.6, \end{cases} \quad (31)$$

where  $D_b$  is the bubble equivalent diameter and  $L_{max}$  is defined as,

$$L_{max} = (\sqrt{2}P_0 - 2R_0) \quad (32)$$

The  $L_{max}$  parameter has been chosen to replace the standard pipe diameter since it corresponds to the maximum bubble size. The bubble larger than  $L_{max}$  will be deformed by the sub-channel walls. Its value depends on the non-dimensional rod diameter and it corresponds from 1.3 to 3.6 times the hydraulic diameter if a range of  $D_0/P_0$  between 0.2 and 0.6 is considered.

#### 4. Results and discussion

##### 4.1. Comparison of distribution parameter model with data

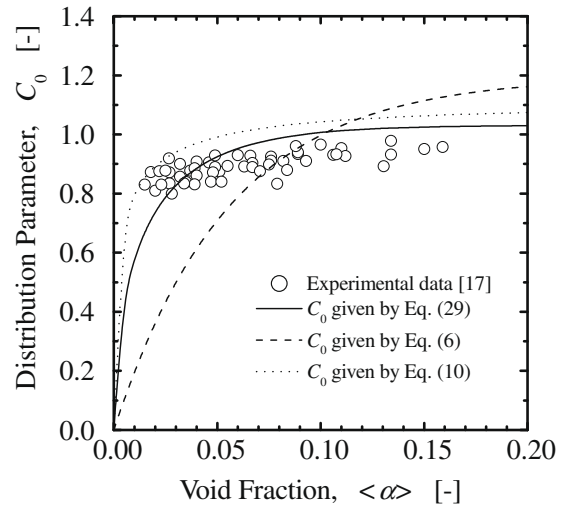
The area-averaged data provided by Yun et al. [17] have been used to check the prediction capabilities of the drift-flux models described in Section 3. In addition, these data have been compared with those obtained by other drift-flux models commonly used in rod bundle geometries and mentioned in Section 1.

Table 3 shows the averaged prediction errors of the constitutive equations of the distribution parameter and drift-velocity developed in Section 3 as well as of the area-averaged void fraction using the constitutive equations and Eq. (3). In the evaluation of the void fraction prediction capability, the existing drift-flux models listed in Table 1 have been considered. Here, we assume that the existing constitutive equations obtained in rod bundles can be applicable to a sub-channel, since the area of corner and wall sub-channels is much smaller than core sub-channels of rod bundles in the experimental facilities that were used for obtaining the correlations (see Table 2). The prediction error is defined as

$$E[\%] = \frac{|(\text{measured value}) - (\text{calculated value})|}{(\text{measured value})} \times 100. \quad (33)$$

**Table 3**  
Prediction accuracy of drift-flux models.

Models	Averaged error $C_0$	Averaged error $\langle\langle v_{gi} \rangle\rangle$	Averaged error $\langle \alpha \rangle$
<i>Distribution parameter</i>			
Eq. (29) with $D_0/P_0 = 0.5$	±8.01%	–	–
<i>Drift velocity</i>			
Eq. (30) with $B_{sf} = 1$ (Ishii's Eq.)	–	±19.6%	–
Eq. (30)	–	±13.1%	–
<i>Drift-flux model</i>			
Eq. (29) with $D_0/P_0 = 0.5$ and Eq. (30) with $B_{sf} = 1$	–	–	±20.4%
Eq. (29) with $D_0/P_0 = 0.5$ and Eq. (30)	–	–	±14.4%
Bestion (1990)	–	–	±23.8%
Inoue et al. (1993)	–	–	±35.1%
Chexal–Lellouche (1992)	–	–	±38.6%
Maier and Coddington (1997)	–	–	±67.6%



**Fig. 7.** Comparison of distribution parameters and experimental data.

Fig. 7 shows the dependence of distribution parameter values on the area-averaged void fraction obtained by Yun et al. [17]. The distribution parameter values in the tested conditions are always lower than 1, which corresponds to the typical wall peaked void fraction profile present in subcooled boiling flow. The distribution parameter is about 0.8 at  $\langle \alpha \rangle = 0.02$  and gradually increases with  $\langle \alpha \rangle$ . Since the distribution parameter is zero at  $\langle \alpha \rangle = 0$  in subcooled boiling flow, very rapid increase in the distribution parameter is expected at  $\langle \alpha \rangle < 0.02$ . The extrapolation of the distribution parameter at higher  $\langle \alpha \rangle$  implies the distribution parameter about 1.04, confirming the results given in Fig. 4(a), since a non-dimensional rod diameter value of  $D_0/P_0 \sim 0.5$  was used in Yun et al. experiments [17].

In addition, in Fig. 7 the distribution parameters obtained (i) in this work for a sub-channel, Eq. (29), (ii) by Ishii's equation [3] for a round pipe, Eq. (6), and (iii) by Hibiki's equation [16] for an internally heated annulus and modified by Ozar et al. [24], Eq. (10), are presented by solid, broken and dotted lines, respectively. The change in the flow channel geometry has a profound impact in the slope of the distribution parameter for void fraction values  $\langle \alpha \rangle$  lower than 0.1. In this way, the slope for the annular channel is six times higher than the one of the round pipe. The rod bundle sub-channel slope is between both the annular and the round pipe ones. This fact seems feasible, since the sub-channel flow geometry can be considered as an intermediate case between the annulus and the round pipe. The agreement between the distribution parameter correlation developed in this work and the experimental data given by Yun et al. [17] seems acceptable. The average predicting error is ±8.01%, a remarkable value since no experimental



data was used in the modeling. Finally, two additional facts need to be considered (i) the data provided by Yun et al. [17] presents some uncertainties, as pointed out in Section 2, especially for low void fraction values due to the lack of measurements near the rod wall and (ii) there is only one available database [17] that provide local data in a rod bundle sub-channel and that, therefore, can be used to check the proposed distribution parameter constitutive equation. It is recommended that the validity of the proposed distribution parameter in the sub-channel is readdressed by additional experimental data, especially for low void fraction values to be obtained in a future study.

4.2. Comparison of drift velocity model with data

In Fig. 8, the drift velocity obtained by the modification of Ishii's equation by the wall effects Eq. (30) and the Ishii's equation [3] (Eq.(30) with  $B_{sf}=1$ ) are indicated by solid and broken lines, respectively. Here, a constant value of  $D_b$  of 1.3 mm has been chosen in Eq. (31), since it is the averaged value of the data used in this study [17]. This fact generates a source of error in the figure, but it is lower than a 10% for all the flow conditions. Consequently, the information given in the figure should be taken for comparative purposes. In the prediction error shown in Table 3 the bubble diameters measured by Yun et al. [17] have been used. However, this information is not usually available in rod bundle assemblies (see Table 2). An alternative approach consists on obtaining the bubble diameter from published correlations in subcooled boiling flow. In this regard, the correlation given by Hibiki et al. [28] provides accurate results with a prediction error of  $\pm 27.1\%$  when it is applied to Yun et al. dataset [17].

As shown in Fig. 8, the void-fraction weighted-averaged drift velocity shows a slight decrease with the void fraction as previously reported in bubbly flow conditions [3,5]. The drift velocity constitutive equations also show this dependence. The results obtained by Eq. (30) provide a prediction error of  $\pm 13.1\%$ . The main source of the error in Eq. (30) is due to the experimental scattering observed in the data [17] that is usual in drift velocity measurements [5]. If the rod wall effect is not considered in Eq. (30),  $B_{sf}=1$ , the prediction error is enlarged to  $\pm 19.6\%$ , which is still acceptable prediction accuracy.

4.3. Comparison of drift-flux model with data

In this section, the prediction accuracy of the area-averaged void fraction is discussed. As shown in Fig. 9, all existing correlations underestimate the void fraction values, except the one developed

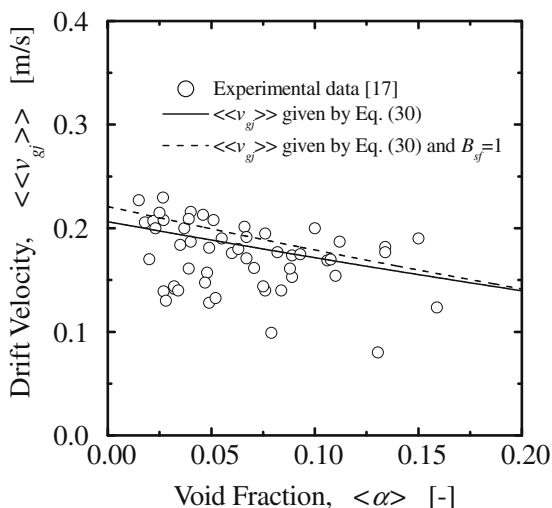


Fig. 8. Comparison of area-averaged drift velocity with experimental data.

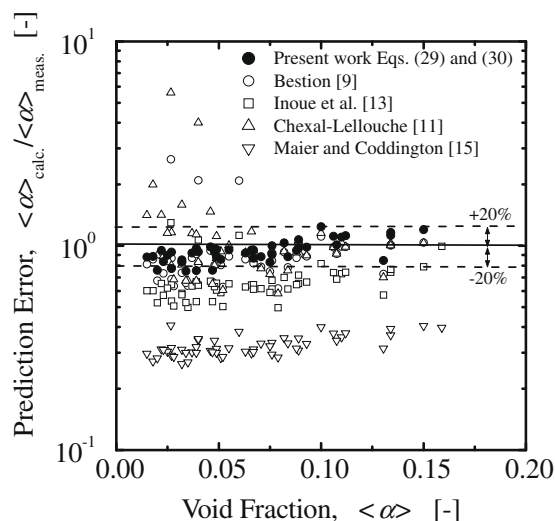


Fig. 9. Comparison of area-averaged void fraction with experimental data.

by Chexal–Lellouche. The compared results by newly developed drift-flux model are highlighted by solid symbols. The lowest prediction error ( $\pm 14.4\%$ ) is obtained by the use of the distribution parameter obtained by the bubble-layer thickness model, Eq. (29) and the drift velocity given by Ishii [3] modified by considering the wall effect, Eq. (30). If no rod wall effect is considered in the drift velocity correlation,  $B_{sf}=1$ , the prediction error is  $\pm 20.4\%$ , still lower than the published correlations considered in this work. In all the correlations, the prediction accuracy is improved for increased area-averaged void fraction where the distribution parameter effect is more pronounced than the drift velocity effect. The results obtained by the Bestion correlations are remarkable since it is a quite simple correlation that is applicable to the whole range of void fractions. However, the Bestion and Chexal–Lellouche correlations present high scattering for low void fraction conditions. The predictions of Inoue et al. and Chexal–Lellouche correlations are similar providing area-averaged void fraction prediction errors lower than  $\pm 40\%$ . The Maier and Coddington correlations do not provide reasonable predictions since the error in the drift velocity estimation is very high.

4.4. Future extension of bubble-layer thickness model to other sub-channel

The constitutive equations obtained in this work are only valid for the center sub-channel type and future work is needed to extend the model to the other sub-channel types (side and corner sub-channels) and, thus, to obtain a better accuracy in the model. However, the side and corner sub-channel types are important in small size rod bundle assemblies. For example, if the non-dimensional rod diameter given in Fig. 1(a) is considered, the flow area covered by the center sub-channel type represents the 44.4%, 56.3% and 76.6% of the total flow area in a  $3 \times 3$ ,  $4 \times 4$  and  $8 \times 8$  rod bundle assembly, respectively. The distribution parameter presents an important dependence on the channel geometry and major differences are expected for the sub-channel types. No local experimental data is available for the corner and side sub-channel types, so only the approach following the bubble-layer thickness model seems to be possible. The drift velocity for the different sub-channel types should be also examined carefully.

5. Conclusions

In this paper, new constitutive equations for the drift-flux model developed for subcooled boiling bubbly flow in a rod bundle sub-

channel are presented and analyzed. In the case of the distribution parameter, its asymptotic value,  $C_{0,\infty}$ , has been obtained analytically. In addition, its dependence on the exponent of the  $j$ - and  $\alpha$ -distributions and the non-dimensional rod diameter value,  $D_0/P_0$ , has been considered and discussed. A correlation for the constitutive equation for subcooled boiling flow in a sub-channel is obtained from the bubble-layer thickness model. In this derivation an existing constitutive equation for subcooled boiling flow in a round pipe [3] is modified by taking account of the difference in the flow channel geometry between the sub-channel and round pipe. In the case of the drift velocity the expression given by Ishii [3] for round pipes is modified in order to consider the rod wall effects.

The area-averaged data obtained by Yun et al. [17] integrated over the whole sub-channel have been used to validate the distribution parameter and drift velocity constitutive equations. In addition, the area-averaged void fraction results provided by the developed constitutive equations have been checked with the most used correlations found in literature.

- Distribution parameter: the averaged relative prediction error by the newly developed correlation based on the bubble-layer thickness model presents a remarkable low prediction error of  $\pm 8.01\%$ . However, more experimental data, especially for low void fraction values, is needed to make a further evaluation.
- Drift velocity: the best prediction results are provided by the Ishii's correlation modified in order to take into account the wall effect with an averaged prediction error of  $\pm 13.1\%$ . If this effect is not considered the prediction error given by the mentioned equation is  $\pm 19.6\%$ .
- Void fraction: the predicting errors provided by the existing correlations are lower than  $\pm 40\%$  (except for the Maier and Coddington correlation) and the best results among them are obtained using the Bestion correlation with a prediction error of  $\pm 23.8\%$ , however, this correlation presents major scattering for low void fraction conditions. Using the distribution parameter distribution developed in this work and the drift velocity constitutive equation given by Ishii it is possible to reduce the prediction error to  $\pm 20.4\%$ . Finally, if the rod wall effects in the drift velocity are taken into account the prediction error can be reduced to  $\pm 14.4\%$ .

## References

- [1] G. Espinosa-Paredes, A. Nuñez-Carrera, SBWR model for steady-state and transient analysis, Science and Technology of Nuclear Installations 2008 (2008), Article ID 428168.
- [2] N. Zuber, J.A. Findlay, Average volumetric concentration in two-phase flow systems, J. Heat Transfer 87 (1965) 453–468.
- [3] M. Ishii, One-dimensional drift-flux model and constitutive equations for relative motion between phases in various two-phase flow regimes, ANL-77-47, USA, 1977.
- [4] M. Ishii, T. Hibiki, Thermo-fluid Dynamics of Two-phase Flow, Springer, New York, USA, 2006.
- [5] T. Hibiki, M. Ishii, Distribution parameter and drift velocity of drift-flux model in bubbly flow, Int. J. Heat Mass Transfer 45 (2002) 707–721.
- [6] T. Hibiki, M. Ishii, One-dimensional drift-flux model for two-phase flow in a large diameter pipe, Int. J. Heat Mass Transfer 46 (2003) 1773–1790.
- [7] H. Goda, T. Hibiki, S. Kim, M. Ishii, J. Uhle, Drift flux model for downward two-phase flow, Int. J. Heat Mass Transfer 46 (2003) 4835–4844.
- [8] P. Coddington, R. Macian, A study of the performance of void fraction correlations used in the context of drift-flux two-phase flow models, Nucl. Eng. Des. 215 (2002) 199–216.
- [9] D. Bestion, The physical closure laws in the CATHARE code, Nucl. Eng. Des. 124 (1990) 229–245.
- [10] P. Venkateswararao, R. Semiat, A.E. Dukler, Flow pattern transition for gas-liquid flow in a vertical rod bundle, Int. J. Multiphase Flow 8 (1982) 509–524.
- [11] B. Chexal, G. Lellouche, J. Horowitz, J. Healzer, A void fraction correlation for generalized applications, Prog. Nucl. Energy 27 (1992) 255–295.
- [12] B. Chexal, G. Lellouche, A full range drift-flux correlation for vertical flows (Revision 1), EPRI Report NP-3989-SR, USA, 1986.
- [13] A. Inoue, T. Kurosu, M. Yagi, S. Morooka, A. Hoshida, T. Ishizuka, K. Yoshimura, In-bundle void measurement of a BWR fuel assembly by a X-ray CT scanner: assessment of BWR design void correlation and development of new void correlation, in: Proc. of the ASME/JSME Nuclear Engineering Conference, 1993.
- [14] S. Morooka, A. Inoue, M. Oishi, T. Aoki, K. Nagaoka, H. Yoshida, In-bundle void measurement of BWR fuel assembly by X-ray CT scanner, in: Proc. of ICON-1, Paper 38, 1991.
- [15] D. Maier, P. Coddington, Review of wide range void correlations against an extensive data base of rod bundle void measurements, in: Proc. of ICON-5, Paper 2434, 1997.
- [16] T. Hibiki, R. Situ, Y. Mi, M. Ishii, Modeling of bubble-layer thickness for formulation of one-dimensional interfacial area transport equation in subcooled boiling two-phase flow, Int. J. Heat Mass Transfer 46 (2003) 1409–1423.
- [17] B.J. Yun, G.C. Park, J.E. Julia, T. Hibiki, Flow structure of sub-cooled boiling water flow in a sub-channel of  $3 \times 3$  rod bundles, J. Nucl. Sci. Technol. 45 (2008) 402–422.
- [18] T. Mitsutake, S. Morooka, K. Suzuki, S. Tsunoyama, K. Yoshimura, Void fraction estimation within rod bundles based on three-fluid model and comparison with X-ray CT void data, Nucl. Eng. Des. 120 (1990) 203–212.
- [19] H. Kumamaru, M. Kondo, H. Murata, Y. Kukita, Void-fraction distribution under high-pressure boil-off conditions in rod bundle geometry, Nucl. Eng. Des. 150 (1994) 95–105.
- [20] R. Deruaz, P. Clement, J.M. Veteau, Study of two-dimensional effects in the core of a light water reactor during the ECC's phase following a loss of coolant accident, EUR 10076 EN, Commissariat à l'Énergie Atomique, Centre d'Étude Nucleaires de Grenoble, Service des Transferts Thermiques, Grenoble, France, 1985.
- [21] J. Dreier, G. Analytis, R. Chawla, NEPTUN-III reflooding and boil-off experiments with an LWHCR fuel bundle simulator: experimental results and initial core assessment efforts, Nucl. Technol. 80 (1988) 93–106.
- [22] Y. Anoda, Y. Kukita, K. Tasaka, Void fraction distribution in rod bundle under high pressure conditions, in: Proc. ASME Winter Annual Meeting, Advances in Gas-Liquid Flows, 1990.
- [23] T.M. Anklam, R.F. Miller, Void fraction under high pressure, low flow conditions in rod bundle geometry, Nucl. Eng. Des. 75 (1983) 99–108.
- [24] B. Ozar, J.J. Jeong, A. Dixit, J.E. Juliá, T. Hibiki, M. Ishii, Flow structure of gas-liquid two-phase flow in an annulus, Chem. Eng. Sci. 63 (2008) 3998–4011.
- [25] A. Tomiyama, Y. Nakahara, Y. Adachi, S. Hosokawa, Shapes and rising velocities of single bubbles rising through a inner subchannel, J. Nucl. Sci. Technol. 40 (2003) 136–142.
- [26] G.B. Wallis, One-dimensional Two-phase Flow, McGraw Hill, 1969.
- [27] L.N. Carlucci, N. Hammouda, D.S. Rowe, Two-phase turbulent mixing and buoyancy drift in rod bundles, Nucl. Eng. Des. 227 (2004) 65–84.
- [28] T. Hibiki, T.H. Lee, J.Y. Lee, M. Ishii, Interfacial area concentration in boiling bubbly flow systems, Chem. Eng. Sci. 61 (2006) 7979–7990.